

## NUMERICAL SIMULATION OF LOUVER FIN HEAT EXCHANGERS WITH VORTEX GENERATORS

by

**Kan CAO<sup>a\*</sup>, Bowen YU<sup>a</sup>, Chunlai TIAN<sup>b</sup>, Yaohua YUAN<sup>a</sup>,  
Zhiwei KANG<sup>a</sup>, and Zezi TAN<sup>a</sup>**

<sup>a</sup>School of Energy and Environment, Zhongyuan University of Technology, Zhengzhou, China

<sup>b</sup>Luoyang Ruichang Environmental Engineering Co, Ltd., Luoyang, China

Original scientific paper

<https://doi.org/10.2298/TSCI2503889C>

*This paper proposes a new type of vortex generator fin structure and employs CFD method to simulate the fin structure. It then studies the temperature and flow fields of vortex generator fins and ordinary louver fins, and compares the heat transfer and flow resistance characteristics of the two types of fins. The results indicate that when the Reynolds number is between 100 and 500, the heat transfer factor of the novel fin structure exhibits an increase of 5.05% to 8.35%, while its resistance factor shows a rise of 5.77% to 12.14%. Furthermore, the comprehensive factor of the fin structure demonstrates an enhancement of 3.11% to 4.29%. Additionally, the  $\Omega$  criterion indicates that the distribution of vortices between the fins is uniform, and a longitudinal vortex network is generated between the fins due to the presence of vortex generators. This results in a higher average temperature near the fins compared to ordinary fins, as well as a faster temperature rise. This paper serves as a reference for further research on high-efficiency finned heat exchangers*

Key words: *louver fins with vortex generator, heat transfer, flow resistance, numerical simulation*

### Introduction

The louvered fin heat exchanger is a versatile and efficient component, suited to a range of applications. Its simple structure, high heat transfer efficiency, and light weight make it an ideal choice for automotive air conditioning heat exchangers. The fins of the heat exchanger act to disrupt the air-flow, thereby increasing the heat transfer capability. This results in a higher degree of heat transfer effect even at a certain pressure drop. Consequently, the study of fin coil heat exchangers is of great significance.

A substantial body of research has been conducted on finned heat exchangers. Some scholars have conducted experimental studies, numerical simulations, and other methods to investigate the heat transfer and flow characteristics of louver fins [1]. Furthermore, other scholars have successfully enhanced the heat transfer efficiency of louver fins by modifying their shape or incorporating specific flow disturbance elements into the fins [2-4].

In their study, Yan *et al.* [5] employed the CFD method to examine four distinct fin types, each equipped with a vortex generator. The blades of these generators were triangular in

\* Corresponding author, e-mail: caokan96@163.com

shape, while the rectangular blades were employed in a separate set of experiments. The findings indicated that the fluid mixing and heat exchange in the dead zone and mainstream zone were enhanced, resulting in an overall improvement in performance. Cao *et al.* [6] conducted research on staggered-hole fins under low Reynolds number conditions. Asadi *et al.* [7] conducted simulations and optimization studies on various geometric structures of louver fin heat exchangers, including the louver angle ratio, the louver pitch ratio, and the ratio of the inlet louver length to the outlet louver length. Vortex generators enhance the heat exchange capacity primarily by generating vortices. The theoretical research on the application and identification of vortices has undergone three stages, as outlined in [8]. Among these, the third generation vortex identification methods, such as  $\Omega$  criteria and Liutex, have been defined.

The majority of research on the fins of finned heat exchangers has focused on optimizing the performance of conventional fins [9, 10], as well as on modifying the entire fin row and fin geometry [11]. The research on the role of vortex generators between the fins is relatively limited. This paper proposes a louver fin structure with a vortex generator and analyzes the effect of the vortex generator using the  $\Omega$  criterion. The goal is to provide a reference for the application of vortex generators in louver fins.

### Model introduction

The louvered fin heat exchanger is filled with refrigerant, which condenses when it contacts the tube wall. The heat is transferred through the tube wall to the inclined fins, and the fins transfer the heat to the air flowing through them. Due to its highly symmetric and periodic structure, it is possible to focus on studying a single column, which will simplify the calculations. In order to facilitate further simplification, the following assumptions will be made:

- the air-flow between each set of fins is uniform,
- the fins are made of aluminum and do not deform with temperature changes, and
- the effect of gravity on the heat exchanger is negligible.

The simplified geometric model of the finned heat exchanger is shown in fig. 1, and its various geometric parameters are given in tab. 1.

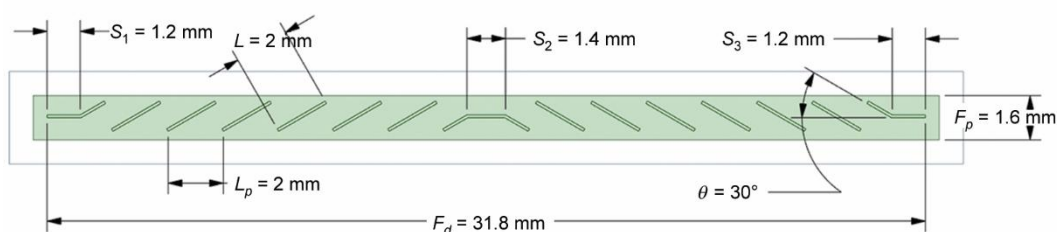


Figure 1. Schematic diagram of the geometric dimensions of the louver fins

Table 1. Basic parameters of ordinary louver fin

Parameter	Value	Parameter	Value
Fin spacing, $F_p$ , [mm]	1.6	Louver angle $\theta$ , [°]	30
Fin length, $L_p$ , [mm]	6.4	Length of inlet fin $L_1$ , [mm]	1.2
Fin height, $F_L$ , [mm]	6.4	Length of turning area, $L_2$ , [mm]	1.4
Fin width, $F_d$ , [mm]	31.8	Length of outlet fin, $L_3$ , [mm]	1.2

The vortex generator louver is obtained by renovating ordinary louver fins as shown in fig. 2. A vortex generator is added between the flow channels formed by ordinary louver fins. The vortex generator is a hemispherical structure with a radius of 0.8 mm.

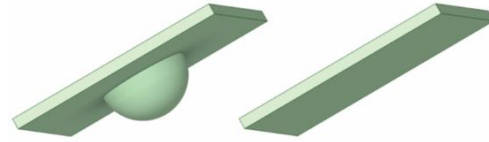


Figure 2. Vortex generator fins and ordinary fins

### Boundary conditions

The specific setting of the boundary conditions for the fin is shown in fig. 3. The left inlet is the velocity inlet with a flow velocity ranging from 0.73 m/s to 3.65 m/s, corresponding to a Reynolds number of 100-500. The inflowing medium is air. The right outlet is the pressure outlet. The upper and lower periodic planes of the linear period are set, and the mesh and parameter settings are the same for each period. The computational domain includes half of the fin and the surrounding fluid domain, with symmetry planes set for both the fluid and the fin. The wall surface in contact with the flat tube is simplified and set to a constant wall temperature surface at 300 K. The surface in contact with the fluid and the fin is set as the fluid-structure interaction surface, and the velocity and pressure are coupled using the SIMPLE algorithm. The laminar flow model is used, and the energy conservation equation and the momentum conservation equation of the second-order welcome style formula are applied.

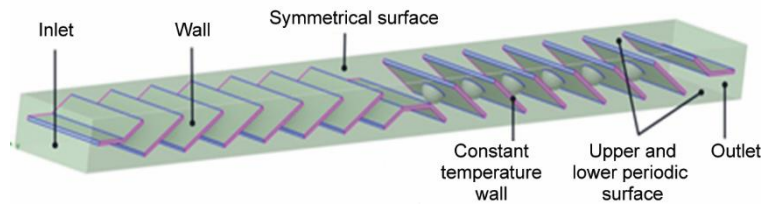


Figure 3. Boundary conditions of louver fin model

### Governing equations

In the absence of significant variations in temperature across the surface of the louver fins and in the physical properties of the air, the fundamental control equations can be established.

– Continuity equation:

$$\frac{\partial \rho}{\partial t} + \frac{\partial (\rho u_i)}{\partial x_i} = S_m \quad (1)$$

– Momentum conservation equation:

$$\frac{\partial (\rho u_i)}{\partial t} + \frac{\partial (\rho u_i u_j)}{\partial x_j} = -\frac{\partial p}{\partial x_i} + \frac{\partial \tau_{ij}}{\partial x_j} + \rho g_i + F_i \quad (2)$$

– Energy equation:

$$\frac{\partial (\rho E)}{\partial t} + \frac{\partial [u_i (\rho E + P)]}{\partial x_i} = \frac{\partial}{\partial x_i} \left[ k_{\text{eff}} \frac{\partial T}{\partial x_i} - \sum_j h_j J_j + u_j (\tau_{ij})_{\text{eff}} \right] + S_h \quad (3)$$

where  $S_m$  is the source,  $P$  – the static pressure,  $\tau_{ij}$  – the stress tensor,  $k_{\text{eff}}$  – the effective thermal conductivity coefficient,  $J_j$  – the combined  $J'$  diffusion flux, and  $S_h$  – the volumetric heat source.

### Evaluation on comprehensive performance

This paper evaluates the performance of fins using heat transfer factor, resistance factor, and combined factor [12]. The equations are:

- Heat transfer factor,  $j$ :

$$j = \frac{h_a}{\rho_a u_a C_{P,a}} \text{Pr}^{2/3} \quad (4)$$

- Resistance factor,  $f$ :

$$f = 2 \frac{\Delta P}{\rho_a u_a^2} \frac{d_e}{L} \quad (5)$$

- Comprehensive factor,  $E_{ij}$ :

$$E_{ij} = \frac{j}{f^{1/3}} \quad (6)$$

where  $h_a$  [ $\text{Wm}^{-2}\text{K}^{-1}$ ] is the heat transfer coefficient on the air side,  $C_{P,a}$  [ $\text{Jkg}^{-1}\text{K}^{-1}$ ] – the heat capacity at constant pressure,  $\text{Pr} = 0.7$ ,  $u_a$  [ $\text{ms}^{-1}$ ] – the incoming velocity of air,  $\rho_a$  [ $\text{kgm}^{-3}$ ] – the air density,  $d_e$  [m] – the equivalent diameter of the model,  $\Delta P$  [Pa] – the pressure at the air outlet, and  $L$  [m] – the length of the air channel of the louver fin model.

The  $\Omega$  criterion calculation formula:

$$\Omega = \frac{\|B\|_F^2}{\|A\|_F^2 + \|B\|_F^2 + \varepsilon} \quad (7)$$

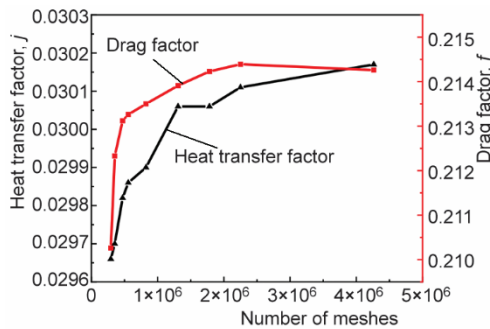


**Figure 4. Effects of grid numbers on the heat transfer factor and drag factor**

grids and using the heat transfer factor,  $j$ , and resistance factor,  $f$ . The results are shown in fig. 4. When the unit size is set to 0.08 mm, the corresponding number of grids is 1782578. At this juncture, the number of grids continues to increase, and the heat transfer factor,  $j$ , and the resistance factor,  $f$ , exhibit minimal variation, thereby corroborating the reliability of grid independence.

where  $\|B\|_F^2$  represents the square of the norm of matrix B, matrix A is the symmetric tensor of the velocity gradient, matrix B is divided into the antisymmetric tensor of the velocity gradient,  $\varepsilon$  – the value greater than 0, which is recommended to be:

$$\varepsilon = \max(\|B\|_F^2 - \|A\|_F^2)/1000.$$

### Grid independence verification

Mesh generation is of paramount importance for numerical simulation. In order to reduce the influence of the number of grids on the simulation results, the grid independence is verified by setting different numbers of

### Numerical simulation verification

The objective of this research is to develop an experimental platform for a heat pump air conditioning system. In order to achieve this objective, an experimental research study is being conducted using a heat exchanger with ordinary louver fins under experimental conditions. The louver fins are connected to the flat tubes of the heat exchanger, and during the experiment, the refrigerant flows through the flat tubes and exchanges heat with the air through the louver fins. The pertinent data pertaining to the heat exchanger is gathered only when the system has met the requisite experimental conditions and is operating in a stable manner.

As illustrated in fig. 5, the resistance factor and heat transfer factor exhibit a comparable trend of change as the Reynolds number increases, with a difference of approximately 2.05% to 24.29% in the heat transfer factor and 13.6% to 15.29% in the resistance factor. This indicates that the performance characteristics of the fin model in the simulation and experiment are consistent. As the dimensions of the experimental fin differ slightly from those of the simulated fin model, the final results exhibit a slight discrepancy. However, the fundamental characteristics remain consistent, and the error falls within the acceptable range of engineering error. The accuracy of the model has been validated.

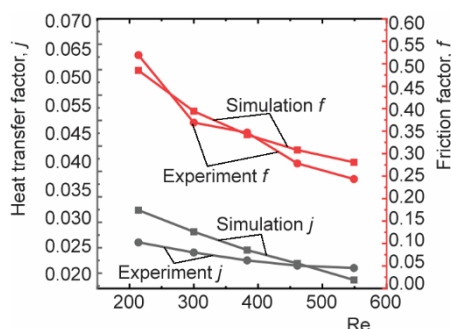


Figure 5. Comparison of experimental and simulated values

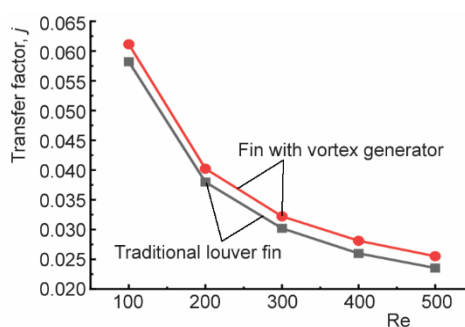


Figure 6. Comparison of heat transfer factors of two fins at different Reynolds numbers

### Analysis of heat transfer characteristics

Figure 6 illustrates the variation of the heat transfer coefficient with Reynolds number for two distinct types of fins. Figure 6 illustrates that the heat transfer coefficient of vortex generators is approximately 5.05% to 8.35% higher than that of ordinary fins. As the Reynolds number increases, the heat transfer coefficient of both types of fins declines, although the rate of this decline becomes less pronounced.

In order to gain a deeper understanding of the influence of vortex generators on fin heat transfer, and given the inclined flow direction of the fluid within the louvered fins, parallel and perpendicular planes to the fins are selected for analysis. The temperature variation is significant at the fourth and fifth fins (including the inlet turning fin) after the fluid enters, and the fluid velocity is relatively fast, which allows for a more detailed examination of the flow and heat transfer near the fins. Accordingly, the fourth and fifth fins are selected for analysis.

As illustrated in fig. 7, the temperature contours of the fins with vortex generators are more concentrated than those of the regular fins, suggesting a more rapid rate of temperature change. In terms of the overall color near the fins, the fins with vortex generators have a higher average temperature. In the local vicinity, the area of the high temperature region of 293 K to

300 K for fins with vortex generators is approximately five to seven times larger than that of ordinary fins, while the area of the low temperature region of 286 K to 288 K is approximately three to five times larger than that of ordinary fins. Consequently, the heat transfer efficiency of louvered fins with vortex generators is demonstrably superior to that of ordinary fins.

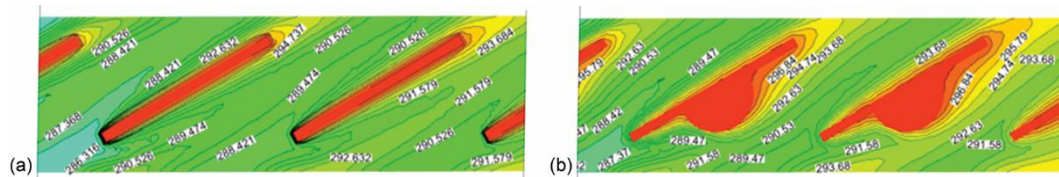


Figure 7. Temperature contours of two types of fins; (a) ordinary louver fins and (b) louver fins with vortex generators

### Analysis of flow resistance characteristics

Figure 8 illustrates the drag coefficient of the fin with a vortex generator and the ordinary fin with a Reynolds number. It can be observed that the drag coefficient of the fin with a vortex generator is approximately 5.77% to 12.14% higher than that of the ordinary fin. As the Reynolds number increases, the drag coefficient of ordinary fins and fins with vortex generators decreases, with the decrease becoming less pronounced.

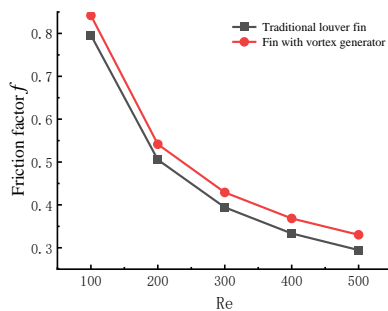


Figure 8. Comparison of heat resistance factors of two fins at different Reynolds numbers

Figure 9 depicts the iso-surfaces diagram calculated by the  $\Omega$  criterion for ordinary fins and fins with vortex generators at the fourth and fifth fins. Figure 9 depicts the iso-surfaces diagram calculated by the  $\Omega$  criterion for ordinary fins 9(a) and fins with vortex generators 9(b). The a1, a2, a3, a4, b1, b2, b3, b4, b5, and b6 symbols represent the vortex regions of ordinary fins and fins with vortex generators, respectively, calculated by the  $\Omega$  criterion. The colors of the two iso-surfaces represent the temperature.

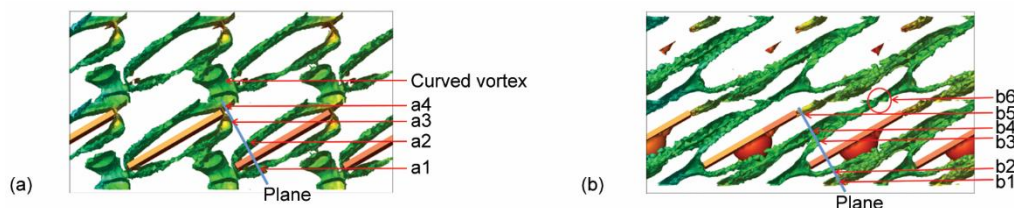


Figure 9. The iso-surface diagram calculated by the  $\Omega$  criterion at the fourth and fifth fins of ordinary fins and fins with vortex generators; (a) ordinary fins and (b) fins with vortex generators

Figure 9(a) illustrates that the vortices generated by ordinary fins are distributed around the fins in a relatively independent manner, with a lower degree of fluid vortex mixing observed in the middle of the fins. In addition, curved vortices are generated between two sets of ordinary fins, which are formed by the fluid between the fin spacing,  $L_p$ , and the fluid between the fin groups,  $F_p$ . As illustrated in fig. 9(a), the curved vortices exhibit a lack of effective

heat transfer surfaces (green color with lower temperature) in their vicinity. However, they do result in pressure loss.

Figure 9(b) illustrates that the vortex generator divides the lower end of the fin (b6) into two longitudinal vortices (b2 and b3). Among these, the longitudinal vortex (b2) and the longitudinal vortex generated by the top end of the previous set of fins (b5 or b1) mix to form a new longitudinal vortex (b4). After a certain distance, the vortex (b6) recombines with the vortices (b2 and b3) generated by the bottom end of the adjacent fins to form a longitudinal vortex. This process is repeated, with the vortex (b6) being divided again by the bottom end of the next set of fins (b2 and b3), forming a network of longitudinal vortices. The longitudinal vortices generated by the fins with vortex generators are distributed uniformly throughout the flow field, forming a network structure with a higher density of longitudinal vortices than ordinary fins.

Figure 10 illustrates the intensity and streamlines of the vortices in the X-axis direction. The cross-section is perpendicular to the direction of the fins and the mainstream of the fluid. Figure 9 illustrates the relationship between the vortex regions observed in fig. 8.

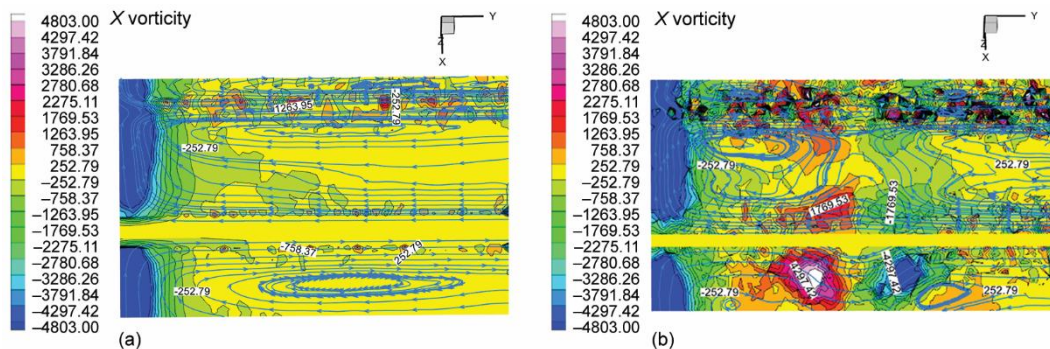


Figure 10. The X-axis eddy current intensity and streamline diagram

Figure 10(b) illustrates that the flow field of the fins with vortex generators is divided into two distinct colors in the middle. This is due to the fact that the vortex generators divide the entire flow field into two longitudinal vortex regions, each with the same intensity but different rotation directions. The intensity and number of small longitudinal vortices generated by the fins with vortex generators at the upper end of the fins are significantly higher than those of ordinary fins. This is caused by the fluid between the fin groups,  $F_p$ , as shown in fig. 9(a). The vortex generators transform the originally transverse curved vortices, which increase flow resistance, into small longitudinal vortices that can significantly enhance heat transfer.

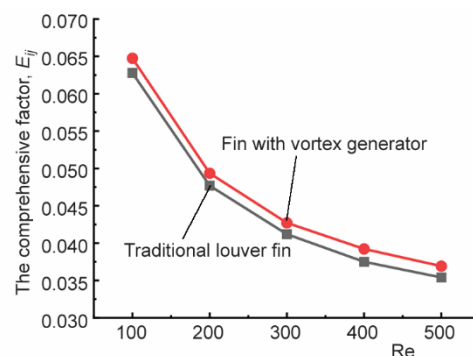


Figure 11. Comparison of heat comprehensive factors of two fins at different Reynolds numbers

Figure 11 presents a comparison of the comprehensive factor for fins with vortex generators and ordinary fins. Although the heat transfer and drag coefficient factors of fins with

vortex generators are higher than those of ordinary fins, as illustrated in fig. 11, the comprehensive factor of fins with vortex generators is still higher than that of ordinary fins by 3.11% to 4.29%. This indicates that fins with vortex generators exhibit superior performance compared to ordinary fins.

## Conclusions

The simulation and analysis of the model with vortex generator fins led to the following conclusions.

- Compared with ordinary fins with vortex generator fins, the heat transfer factor, resistance factor, and integrated factor were found to be improved by 5.05% to 8.35%, 5.77% to 12.14%, and 3.11% to 4.29%, respectively, and the performance of fins with vortex generator is superior.
- The vortex generator introduces disturbances between the fins of the louvered fins. The fins with the vortex generator exhibit a higher average temperature of the fluid at the same location and a faster rate of heat accumulation.
- Computational analyses employing the  $\Omega$  criterion demonstrated that the fins with vortex generators generated a high density of reticulated longitudinal vortices with one another, whereas the conventional fins produced only a modest number of longitudinal vortices in the vicinity of the fins.
- The vortex generator divides the large longitudinal vortex into two smaller longitudinal vortices rotating in opposite directions. The vortex strength of conventional fins in the X-axis direction is constrained to  $\pm 252.79$  and  $\pm 758.37$ , respectively. In contrast, fins with vortex generators can reach vortex strengths of  $\pm 4297.42$  and  $\pm 1769.53$ , with a significant number of smaller longitudinal vortices generated at the upper end of the fins.

## Acknowledgment

This work was supported by the National Natural Science Foundation Project (21776263).

## References

- [1] Dai, L. J., Liu, N., Research Progress on the Influence of Louver Fin Structure on Air-Side Flow and Heat Transfer, *Thermal Power Engineering*, 33 (2018), 5, pp. 1-6
- [2] Cao, K., et al., Numerical Simulation of Heat Exchanger with Perforated Louver Fin, *Cryogenics & Superconductivity*, 49 (2021), 11, pp. 41-46
- [3] Dezan, D. J., et al., Parametric Investigation of Heat Transfer Enhancement and Pressure Loss in Louver Fins with Longitudinal Vortex Generators, *International Journal of Thermal Sciences*, 135 (2019), Jan., pp. 533-545
- [4] Ameel, B., et al., Interaction Effects between Parameters in a Vortex Generator and Louver Fin Compact Heat Exchanger, *International Journal of Heat and Mass Transfer*, 77 (2014), Oct., pp. 247-256
- [5] Yan, K., et al., Improvement of the Performance of Heat Exchanger with Louver Fin Tube by Longitudinal Vortex Generators, *Refrigeration Technology*, 36 (2016), 3, pp. 19-23
- [6] Cao, K., et al., Numerical Analysis of the Flow and Heat Transfer Characteristics of a Staggered Perforated Louver-Finned Heat Exchanger, *Thermal Science*, 27 (2023), 3A, pp. 1855-1863
- [7] Asadi, M., et al., Constructal Optimization of Louver Fin Channels Subjected to Heat Transfer Rate Maximization and Pressure Loss Minimization, *Heat Transfer Engineering*, 39 (2018), 5, pp. 436-448
- [8] Wang, Y. Q., Gui, N., A Review of the Third Generation Vortex Identification Methods and their Applications, *Journal of Hydrodynamics (Series A)*, 34 (2019), 4, pp. 413-429
- [9] Dong, J., et al., Heat Transfer and Pressure Drop Correlations for the Multi-Louver Fin Compact Heat Exchangers, *Energy Conversion and Management*, 48 (2007), 5, pp. 1506-1515

- [10] Giri, S. A., *et al.*, Sizing Analysis of Louver Fin Flat Tube Compact Heat Exchanger by Genetic Algorithm, *Applied Thermal Engineering: Design, Processes, Equipment, Economics*, 125 (2017), Oct., pp. 1426-1436
- [11] Wanglerpanich, K., Kittichaikarn, C., Heat Transfer Efficiency Enhancement Using Zigzag Louver Fin, *Numerical Heat Transfer, Part A: Applications*, 79 (2021), 4, pp. 278-293
- [12] T'Joel, C., *et al.*, Determination of Heat Transfer and Friction Characteristics of an Adapted Inclined Louver Fin, *Experimental Thermal and Fluid Science*, 30 (2006), 4, pp. 319-327